BIOCHEMISTRY
including biophysical chemistry & molecular biology
Article

Biochemistry **2011,** *50,* 1421–1428 1421
DOI: 10.1021/bi1016205

Characterization of the Terminal Activation Step Catalyzed by Oxygenase CmmOIV of the Chromomycin Biosynthetic Pathway from *Streptomyces griseus*[†]

Mary A. Bosserman,[‡] Ana B. Flórez,[§] Khaled A. Shaaban,[‡] Alfredo F. Braña,[§] Jose A. Salas,[§] Carmen Méndez,*[,§] and Jürgen Rohr*[,‡]

[‡]*Department of Pharmaceutical Sciences, College of Pharmacy, University of Kentucky, 789 South Limestone Street, Lexington, Kentucky 40536-0596, United States, and* [§]*Departamento de Biología Funcional e Instituto Universitario de Oncología del Principado de Asturias (IUOPA), Universidad de Oviedo, 33006 Oviedo, Spain*

Received October 7, 2010; Revised Manuscript Received January 17, 2011

ABSTRACT: Inactivation and initial interrogation of key oxygenase CmmOIV of the biosynthetic pathway of chromomycin A_3 in *Streptomyces griseus* ssp. *griseus* revealed that a completely methylated and acetylated prechromomycin is the preferred substrate of this enzyme. This suggests that the three sugar decoration reactions, two O-acetylations and an O-methylation, which were previously believed to occur as the final steps of chromomycin A_3 biosynthesis, indeed take place prior to the CmmOIV reaction. Upon inactivation of CmmOIV, four new compounds accumulated; the fully decorated prechromomycin and its incompletely acetylated precursor along with a diketoprechromomycin-type compound were fully characterized and assayed with CmmOIV.

Chromomycin A_3 **9** (Scheme 1) is a member of the aureolic acid family of antitumor antibiotics that also includes mithramycin (**7**), olivomycin, durhamycin A, UCH9, and chromocyclomycin (*1*, *2*). Aureolic acids act on Gram-positive bacteria and inhibit the growth and multiplication of several cancer cell lines by interacting in a Mg^{2+}-dependent manner with GC-rich regions of the minor groove of DNA (*3*, *4*). Durhamycin A is also an inhibitor of HIV[1] Tat transactivation (*5*). Additionally, chromomycin and mithramycin are strong inducers of erythroid differentiation in K562 cells and potent inhibitors of neuronal apoptosis, making these compounds candidates for therapeutics of hematological diseases and neurological disorders, respectively (*6*). Chromomycin A_3 and mithramycin can also inhibit Zn^{2+} metalloenzymes, including alcohol dehydrogenase (ADH), by binding at the zinc centers and disrupting the quaternary structure of the metalloenzyme complex. This activity makes chromomycin A_3 and mithramycin potential therapeutics for metal dyshomeostasis and neurodegenerative disorders (*7*).

Chromomycin A_3 **9** and all other aureolic acid compounds (except chromocylomycin) contain a tricyclic chromophore with two oligosaccharide chains attached via *O*-glycosidic bonds at positions C-2 and C-6 of the aglycone as well as two aliphatic side chains at C-3 and C-7 (Scheme 1). The aglycone is formed by condensation of one acetyl-CoA and nine malonyl-CoA units and belongs to the polyketide group of natural products (*8*−*11*). In each aureolic acid compound except UCH9 and durhamycin A, the oligosaccharides at C-2 and C-6 are di- and trisaccharide chains, respectively, and contain unique deoxyhexose sugars for each of the aureolic acid compounds. The disaccharide chain of chromomycin A_3 contains 4-*O*-acetyl-D-oliose (sugar A) and 4-*O*-methyl-D-oliose (sugar B), while the trisaccharide chain contains two D-olivoses (sugars C and D) and 4-*O*-acetyl-L-chromose B (sugar E). Four glycosyltransferase enzymes (CmmGI, -GII, -GIII, and -GIV) encoded in the chromomycin A_3 gene cluster glycosylate the aglycone precursor premithramycinone, starting with the buildup of the trisaccharide chain followed by the generation of the disaccharide (*10*). Two tailoring enzymes are responsible for the transfer of acetyl and methyl groups to the sugars, CmmA and CmmMIII, respectively (*8*). Both the sugars and their acetyl groups contribute to the biological activity of chromomycin A_3 (*3*, *4*, *12*−*25*).

The biosyntheses of mithramycin and chromomycin A_3 progress through common intermediates, up to premithramycin A_1 **3**, and then differ with regard to the assembly of their remaining saccharide patterns (Scheme 1). Consequently, both compounds share a common aglycone but are each glycosylated with a unique pattern of sugars. In addition, the decoration of the sugar moieties of chromomycin A_3 with two acetyl groups and one methyl group distinguishes chromomycin A_3 from mithramycin biosynthesis. To date, the exact timing of these decoration reactions within the chromomycin A_3 biosynthesis remains ambiguous. Previously, we proposed the acetyl and methyl transfers catalyzed by CmmA and CmmMIII, respectively, were the terminal steps in chromomycin A_3 biosynthesis, based on gene inactivation studies and the likelihood that CmmA was embedded in the cell membrane (*8*, *26*). The isolation of compounds from inactivation of CmmA and CmmMIII yielded chromomycin A_3 derivatives with missing acetyl and methyl decorations, and the dideacetylchromomycin A_3 appears to be a substrate for the out-transporters CmrA and CmrB (*26*). On the other hand, mutants in which

[†]This work was supported by a grant from the National Institutes of Health (Grant CA 091901) to J.R. and Grant BIO2008-00269 from the Spanish Ministry of Science and Innovation to C.M.

*To whom correspondence should be addressed: Department of Pharmaceutical Sciences, College of Pharmacy, University of Kentucky, 789 S. Limestone St., Lexington, KY 40536-0596. Phone: (859) 323-5031. Fax: (859) 257-7564. E-mail: jrohr2@email.uky.edu.

[1]Abbreviations: ADH, alcohol dehydrogenase; HIV, human immunodeficiency virus; PCR, polymerase chain reaction; UPLC, ultra-high-performance liquid chromatography; HPLC, high-performance liquid chromatography; DMSO, dimethyl sulfoxide; LB, Luria-Bertani; IPTG, isopropyl β-D-1-thiogalactopyranoside; IMAC, immobilized metal ion affinity chromatography; Tris, tris(hydroxymethyl)aminomethane; TBE, Tris/borate/EDTA; MS, mass spectrometry; HRMS, high-resolution mass spectrometry; NMR, nuclear magnetic resonance; ESI-MS, electrospray ionization mass spectrometry; HRESI-MS, high-resolution electrospray ionization mass spectrometry.

Published on Web 01/18/2011

Scheme 1: Biosynthetic Pathways toward Mithramycin in *Streptomyces argillaceus* and Chromomycin A_3 in *Streptomyces griseus* ssp. *griseus*[a]

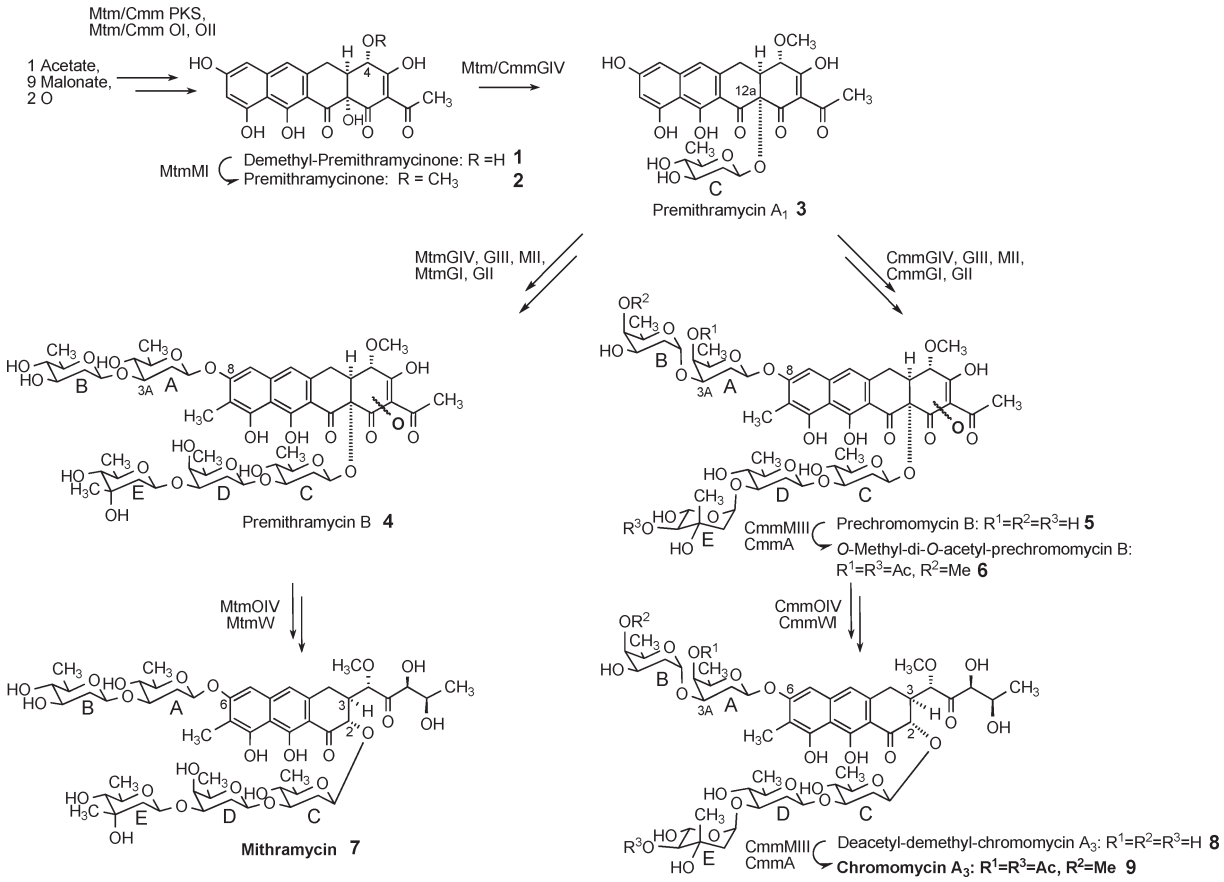

[a]For the chromomycin A_3 specific pathway, ambiguity about whether the sugar unit decorating enzymes CmmMIII and CmmA act before (**5** → **6** → **9**) or after (**5** → **8** → **9**) the oxidative breakage of the fourth ring through CmmOIV exists.

glycosyl transfer steps affecting sugar units B alone or both A and B were inactivated and yielded still tricyclic tetrasaccharidal and tetracyclic trisaccharidal prechromomycins with already O-acetylated sugar moieties A and/or E (*10*). While these contradictive results could be explained by substrate flexibility of the sugar decorating enzymes, a potential substrate flexibility of key oxygenase CmmOIV is an alternative. CmmOIV, in analogy to MtmOIV (*27*) in the well-studied mithramycin biosynthesis, is proposed to catalyze the oxidative rearrangement of a fully sugar-decorated prechromomycin-type compound (**5** or **6**) into a chromomycin-type compound (**8** or **9**) (*9*). A certain substrate flexibility may allow this conversion to occur with or without the *O*-acetyl and *O*-methyl sugar decorations in place, thus leaving unanswered the question of whether the O-acetylation and/or the O-methylation reactions occur prior to or after the CmmOIV reaction (Scheme 1, either **5** → **6** → **9** or **5** → **8** → **9**). In this study, we aimed to further clarify these late steps of chromomycin biosynthesis by exploring oxygenase CmmOIV and its substrate specificity.

EXPERIMENTAL PROCEDURES

Generation of the cmmOIV-Minus Mutant Streptomyces griseus C60O4. For the generation of a *cmmOIV*-minus mutant, plasmid pABF10 was constructed as follows (Figure S1 of the Supporting Information). A 4.77 kb *Pst*I−*Bsp*QI fragment (blunt-ended) of cosGR60, containing *cmmMI*, *cmmGI*, *cmmOIV*, *cmmWI*, and the 5′-end of *cmmLI*, was subcloned into the *Sma*I site of pIJ2925, generating pABF8. Then, a *Sma*I−*Eco*RV fragment obtained from pEFBA (*28*), containing an apramycin resistance cassette, was inserted into the unique *Bsm*I site (blunt-ended) of pABF8 located within *cmmOIV*, and in the same direction of transcription, generating pABF9. Afterward, the whole insert was rescued from pABF9 as a *Bgl*II fragment (using these sites from the poly linker) and subcloned into the *Bam*HI site of pHZ1358, generating pABF10. This construct was introduced by intergeneric conjugation into *S. griseus*, and apramycin-resistant thiostrepton-sensitive transconjugants were selected for further characterization by PCR analysis, using oligonucleotides *cmmOIV-f* (5′-ATGG-AGTACGACGTCGTCGTGGC-3′) and *cmmOIV-r* (5′-GGAA-CGTCCTTCTCCGGAAGTGT-3′). PCR was performed in 50 μL volumes containing 10 mM Tris-HCl, 50 mM KCl, 1.5 mM $MgCl_2$, 2 mM $MgSO_4$, NTPs (0.2 mM each), 0.2 mM primers, 1.5 units of Taq polymerase (Roche Diagnostics), and 2 μL of DNA. The amplification reaction was performed under the following conditions: initial denaturation for 5 min at 98 °C; 35 cycles of 1 min at 98 °C, 1 min at 50 °C, and 2 min at 72 °C; and an extra extension step for 5 min at 72 °C.

HPLC Analysis and Purification of the New Compounds. Chromatographic analyses were performed by UPLC or HPLC-MS as previously described (*29*), except that bidimensional chromatograms were extracted at 280 nm. For the purification of new compounds produced by mutant C60O4, this strain was inoculated from solid agar plates with R5A solid medium into 500 mL of R5A liquid medium in 13 Erlenmeyer flasks (2 L). A total of 7.5 L of medium was used for cultures,

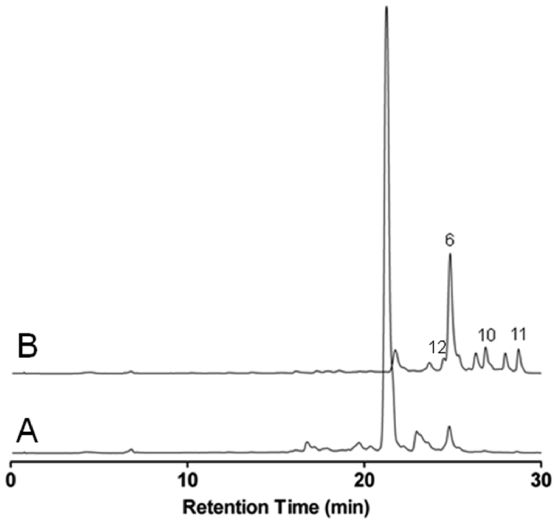

FIGURE 1: HPLC chromatogram traces of wild-type (A) and mutant (B) strains measured at 420 nm.

which were incubated at 28 °C for 5 days with shaking at 250 rpm. Culture broth was harvested and extracted three times with ethyl acetate. The extract obtained after evaporation of the solvent was dissolved in 25 mL of methanol, and the compounds of interest were purified by preparative HPLC with a SunFire C18 column (10 mm × 250 mm, Waters), using mixtures of acetonitrile and 0.2% formic acid in water as solvents, at a flow rate of 2.5 mL/min. The solutions obtained were partially evaporated to reduce the concentration of the organic solvent and finally lyophilized. The final yields were 28.0, 2.4, 1.3, and 1.0 mg of **6**, **12**, **11**, and **10**, respectively (Figure 1).

Cloning of the cmmOIV Gene in pET28a. From plasmid pABF8, *cmmOIV* was amplified via a two-round cloning procedure. Primers were optimized using Primer Quest (IDT, Coralville, IA) upstream and downstream of the start and stop codons of the cmmOIV gene. Amplification of this product using Pfu polymerase (Stratagene) yielded a template for a subsequent amplification using Pfu (Stratagene) and primers with *Nde*I and *Eco*RI restriction sites immediately upstream and downstream of the start and stop codons, respectively (Table 1). The blunt-ended amplification product was then ligated into the pCRBluntII-TOPO vector with the TOPO cloning kit (Invitrogen), transformed into TOP10 cells (Invitrogen), and plated on LB medium with 50 μg/mL kanamycin sulfate overnight at 37 °C. The *cmmOIV* gene was cut from pCRBluntII-TOPO with *Nde*I and *Eco*RI and ligated into freshly digested pET28a (Novagen), resulting in pET-CmmOIV with an N-terminal His_6 tag, and then transformed into XL1-Blue cells. Single colonies were grown in 5 mL of LB medium, and plasmid DNA was isolated (Fermentas) and confirmed by sequencing (SeqWright, Houston, TX). Finally, a transformation of pET-CmmOIV into *Escherichia coli* BL21(DE3) cells for protein production was performed, and 50% glycerol was added for storage at −80 °C.

Expression and Purification of CmmOIV. Glycerol stocks of pET-CmmOIV in BL21(DE3) cells were grown in fresh LB medium in the presence of kanamycin sulfate (50 μg/mL); 250 mL flasks with 100 mL of LB medium with Kan were inoculated with 3 mL of CmmOIV preculture and grown at 37 °C and 250 rpm and then induced when the OD_{600} reached 0.5−0.7 with 1 mM IPTG. Cultures were grown overnight at 18 °C and 250 rpm. Harvested cultures were spun at 4000K rpm for 15 min at 4 °C.

Table 1: Oligonucleotide Primers for *cmmOIV* Cloning

primer name	sequence
*cmmOIV*_reverse	5′-TTCGAGACCTTCACGGACGTGTTT-3′
*cmmOIV*_forward	5′-TGGACATGTTCCTGGTCCCGA-3′
*cmmOIV_Nde*I	5′-AATTATCATATGGAGTACGACGTCG-3′
*cmmOIV_Eco*RI	5′-AATGAATTCTACCTCCCGTCCTGG-3′

Ten milliliters of lysis buffer [50 mM NaH_2PO_4, 300 mM NaCl, and 10 mM imidazole (pH 8.0)] was added to ∼5 g of bacterial cells and resuspended before being lysed by two passes through a French press. Lysed cells were spun at 18000 rpm for 45 min, and then the supernatant was filtered through a 0.45 μm syringe filter. Purified protein was collected by being passed across IMAC purification and P-6 desalting columns (Bio-Rad) using a Profinia purification system (Bio-Rad) and a standard IMAC purification protocol. Approximately 10 mg/L soluble CmmOIV was produced. Protein concentrations were determined by the Bradford assay (Sigma).

Polyacrylamide Gel Analysis. Both native and denaturing gels were run to validate the molecular weight and assay for quaternary structure in solution. CmmOIV was run on a 10% native gel in 1× TBE, while the 10 to 16% SDS−PAGE gel (Bio-Rad) was run in 1× Tris/glycine/SDS buffer.

Gel Filtration Experiments. A molecular weight standard kit (Sigma) was used to establish a standard curve. Molecular weight standards (blue dextran, bovine serum albumin, cytochrome *c*, alcohol dehydrogenase, β-amylase, and carbonic anhydrase) were run across a Superose 12 10/300 GL (Amersham Biosciences) column by FPLC (Bio-Rad), and elution times were monitored. Elution and void volumes were calculated from the elution times, and a standard curve was plotted from the volumes and molecular weights of these proteins. CmmOIV was also run across the column, and an elution time was recorded and used for the determination of the molecular weight of the enzyme. Each protein (∼200 μL) was run across the column in crystallization buffer [20 mM Tris (pH 7.5) and 200 mM NaCl] at a flow rate of 0.5 mL/min.

CmmOIV Activity Assays. CmmOIV assays were conducted as described previously for MtmOIV (*27*). In brief, 1 μM enzyme was combined with 250 μM NADPH, 100 μM FAD, 100 mM Tris (pH 8.25) (unless otherwise noted), and 0−200 μM substrate in a 120 μL reaction mixture. Reaction turnover was assessed by NADPH oxidation and was monitored by continuous absorbance measurements at a λ of 340 nm and 30 °C for up to 30 min.

RESULTS

Insertional Inactivation of cmmOIV. Analysis of the chromomycin A_3 gene cluster of *S. griseus* subsp. *griseus* revealed significant similarity to the related mithramycin gene cluster. One of these genes, *cmmOIV*, is highly similar in sequence to *mtmOIV*, which encodes a FAD-dependent Baeyer−Villiger monooxygenase responsible for the oxidative cleavage of the fourth ring of premithramycin B (*9*). To determine its specific role in chromomycin A_3 biosynthesis, we inactivated *cmmOIV*. A construct in unstable plasmid pHZ1358 was generated (pABF10), in which the *cmmOIV* gene was interrupted by an apramycin resistance cassette inserted in the direction of transcription of the targeted gene (Figure S1A of the Supporting Information). This construct was introduced into *S. griseus* by intergeneric conjugation from

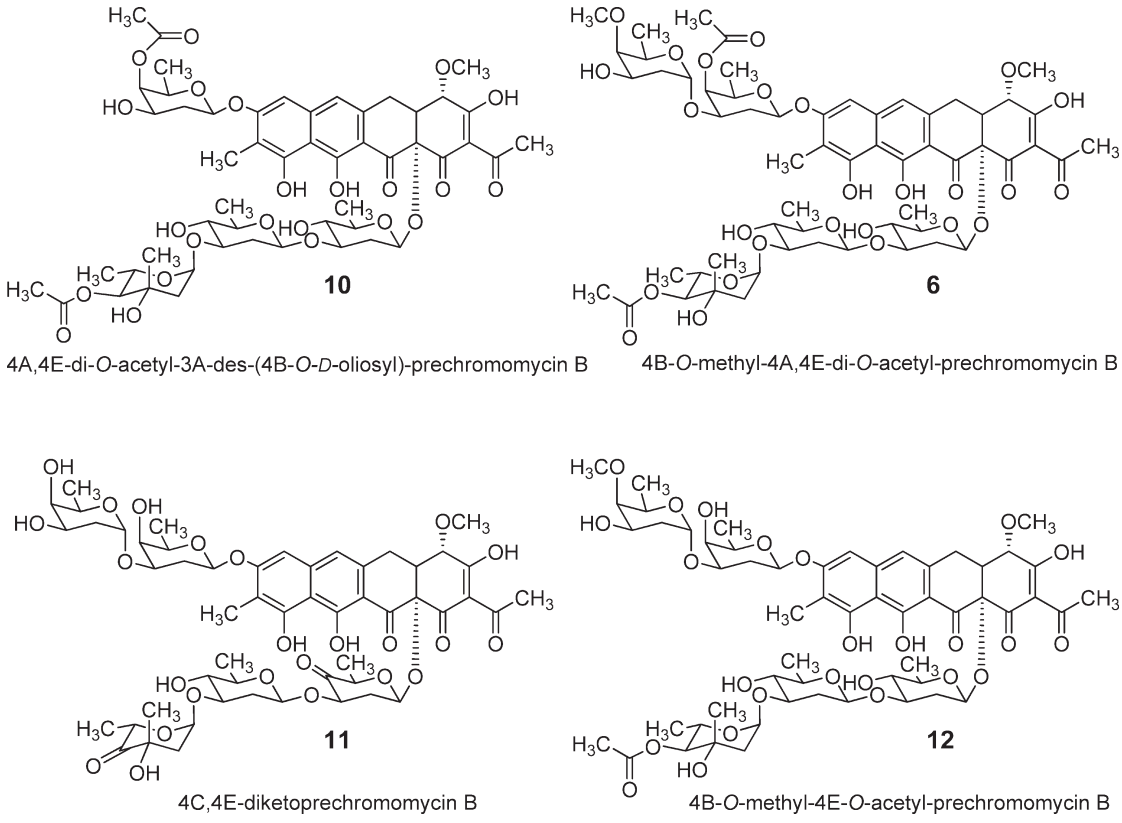

FIGURE 2: Suggested chemical structures of the four isolated products of the CmmOIV-minus mutant, C60O4.

E. coli; transconjugants were selected for resistance to apramycin and then tested for their susceptibility to thiostrepton as a consequence of a double crossover. One mutant (C60O4) was selected and characterized by PCR analysis to verify the occurrence of the double recombination event (Figure S1B of the Supporting Information). Using specific oligonucleotide primers, a 0.57 kb fragment of *cmmOIV* was amplified in the wild-type strain, while a 2.17 kb fragment was amplified in the mutant C60O4, confirming the replacement.

The mutant was further characterized for production of chromomycin A_3 (or derivatives) by UPLC and HPLC-MS analysis. No chromomycin A_3 was detected in extracts of the mutant, indicating the involvement of *cmmOIV* in chromomycin A_3 biosynthesis. Analysis by HPLC of cultures of C60O4 showed one major peak and three minor peaks. The peaks were identified as tetracyclic prechromomycin-type compounds based on a hallmark UV absorption spectrum.

Isolation and Elucidation of Structures of Novel Compounds That Accumulate in the CmmOIV-Minus Mutant. The new compounds produced by mutant C60O4 were purified by preparative HPLC from cultures grown in liquid R5A medium. HRMS analysis of each of the four mutant products yielded molecular weights that allowed preliminary identification of the compounds (Figure 2). The HRMS of **10**, a minor compound of which ~1 mg was isolated, yielded a mass that indicated a molecular formula of $C_{51}H_{66}O_{23}$, which corresponds to a prechromomycin-type compound with only four sugars rather than the normal five. The mass difference compared to the fully decorated 4B-*O*-methyl-4A,4E-di-*O*-acetyl-prechromomycin B **6** (see below and Figure 2) indicated that the *O*-methylated sugar B is missing, which in fact is the last sugar attached during chromomycin A_3 biosynthesis. Thus, its structure is likely 4A,4E-di-*O*-acetyl-3A-des-(4B-*O*-methyl-D-oliosyl)-prechromomycin B **10**. This minor compound is possibly a shunt product derived from the tetrasaccharidal prechromomycin intermediate of chromomycin biosynthesis.

The HRMS of product **6**, consistent with a molecular formula of $C_{58}H_{78}O_{26}$, indicates a fully decorated prechromomycin derivative, with all five sugars and both the *O*-methyl and the two *O*-acetyl groups attached at sugars B, A, and E, respectively. Thus, HRMS putatively identified compound **6** as 4B-*O*-methyl-4A, 4E-di-*O*-acetyl-prechromomycin B, and 28.0 mg of **6** was isolated from the major peak of the CmmOIV-minus mutant strain (Figure 1).

HRMS analysis of **11** indicated a molecular formula of $C_{53}H_{68}O_{24}$, consistent with a diketo-prechromomycin B structure. The structure of **11** matches earlier discussions that concluded that CmmGIV, the glycosyltransferase responsible for the transfers of both sugars A and E, actually transfers 4-keto sugars, which are reduced after the attachment, presumably by CmmTIII (*10*). Thus, compound **11** might indeed be an (unstable) intermediate of the chromomycin A_3 biosynthetic pathway.

Product **12** was separated as a very minor "contaminant" from the main product peak (2.4 mg). The HRMS of **12**, consistent with a molecular formula of $C_{56}H_{76}O_{25}$, indicates a monoacetylated, methylated prechromomycin B product and was putatively identified as 4B-*O*-methyl-4E-*O*-acetyl-prechromomycin B **12**. Similar to compounds **6** and **11**, **12** is possibly an intermediate of chromomycin A_3 biosynthesis, an immediate precursor of **6**. This is consistent with earlier conclusions in that the 4E-*O*-acetyl transfer occurs prior to the 4A-*O*-acetyl transfer (*8*).

For NMR analysis, we could isolate only compounds **6**, **11**, and **12** in sufficient quantities.

4B-O-Methyl-4A,4E-di-O-acetyl-prechromomycin B (**6**). Compound **6** was obtained as an UV-absorbing yellow solid of

Table 2: Physicochemical Characterization of the Four Isolated Compounds from CmmOIV-Minus Mutant Strain C60O4

	10	**6**	**11**	**12**
appearance	yellow solid	yellow solid	yellow solid	yellow solid
R_f (CH_2Cl_2/5% MeOH)	–	0.34	0.36	0.32
(−)-ESI-MS	1045 $[M - H]^-$	1189 $[M - H]^-$	1087 $[M - H]^-$	1147 $[M - H]^-$
(+)-ESI-MS	–	1213 $[M + Na]^+$	1111 $[M + Na]^+$	1171 $[M + Na]^+$
(−)-HRESI-MS	1045.3926 $[M - H]^-$	1189.4708 $[M - H]^-$	1087.4040 $[M - H]^-$	1147.4613 $[M - H]^-$
calcd	1045.3922 for $C_{51}H_{65}O_{23}$	1189.4708 for $C_{58}H_{77}O_2$	1087.4028 for $C_{53}H_{67}O_{24}$	1147.4603 for $C_{56}H_{75}O_2$

medium polarity. The physicochemical properties are summarized in Table 2. The molecular weight was determined by ESI-MS: one quasi-molecular ion peak in negative ESI-MS mode confirmed the molecular weight of **6** as 1190, and negative mode HRESI-MS delivered the molecular formula $C_{58}H_{78}O_{26}$. The UV data and ^{1}H NMR spectrum indicated similarity with premithramycin B **4** (*30*) with respect to the aglycone moiety and with chromomycin A_3 **9** (*9*) with respect to the sugars (Table S1 of the Supporting Information).

The comparison of NMR data revealed that the polyketide-derived aglycone moiety of **6** is identical to that of premithramycin B, while its sugar pattern is the same as that found in chromomycin A_3. Comparing the aglycone data to those of chromomycin A_3 showed that the oxymethines in chromomycin A_3 at δ 4.96 (2-H, d, J = 12 Hz) and δ 4.85 (4′-H, dq, J = 6.5, 3 Hz) were missing and replaced with two quaternary carbons (δ 78.0 and 201.3) of C-12a and C-1′ in **6**. Furthermore, the doublet methyl at δ 1.60 (C-5′, d, J = 6.5 Hz) of chromomycin A_3 was replaced by the singlet at δ 2.72 (C-2′), indicating its attachment at an sp^2 carbon in compound **6**. From the HMBC and ^{1}H−^{1}H COSY correlations of **6** (Figure S2 of the Supporting Information), the final structure was deduced and named 4B-*O*-methyl-4A,4E-*O*-diacetyl-prechromomycin B **6**. The absolute stereochemistry of **6** was deduced on the basis of NOESY experiments (Figure S3 of the Supporting Information) and coupling constants and in comparison with the related chromomycin A_3 (*9*) and premithramycin B (*30*). The coupling constants of the anomeric protons in sugars A, C, and D (J = 9.6−10.1 Hz), indicating its axial orientation, as in chromomycin A_3, and the anomeric protons of the remaining two sugars B and E (J = 2.9−3.2 Hz) indicated their equatorial orientations. Thus, the sugar residues were linked as in chromomycin A_3.

4C,4E-Diketoprechromomycin B (***11***). Compound **11** was isolated as yellow solid and exhibits physicochemical properties similar to those of **6** and **12** (Table 2). The molecular formula $C_{53}H_{68}O_{24}$ determined by HRESI-MS (m/z 1087.4028 $[M - H]^-$) differs from that of **6** by $C_5H_{10}O_2$. Comparison of the ^{1}H and ^{13}C NMR spectra of **6** and **11** (Table S2 of the Supporting Information) revealed that the signals of the two acetyl groups and of the sugar-B methoxy signal in compound **6** were missing in the spectra of **11**. The remaining 4H difference was due to the oxidation at positions of 4C and 4E of the sugar residues, which also can be observed in the NMR spectra (Table S2 of the Supporting Information), which lack the 4-H signals of sugars C and E. Note that the carbonyl signals could not be observed in the ^{13}C NMR spectrum of **11** because of the small quantities that can be isolated. In summary, compound **11** was identified as 4C,4E-diketoprechromomycin B.

4B-O-Methyl-4E-O-acetyl-prechromomycin B (***12***). In the same way, **12** was obtained as an UV-absorbing yellow solid, slightly more polar than **6** (Table 2). The molecular weight was determined by negative mode ESI-MS as 1148; negative mode HRESI-MS delivered the molecular formula $C_{56}H_{76}O_{25}$ (42 amu lower than that of **6**), indicating a loss of one of the two acetyl groups. The ^{1}H NMR spectrum of **12** was very similar to that of **6**, the sole difference being the absence of the singlet methyl at δ 2.09 (4A-OAc) found in **12**. Thus, the 4-*O*-acetyl-β-D-oliose (sugar A) of **12** was replaced with β-D-oliose, and the structure was identified as 4B-*O*-methyl-4E-*O*-acetyl-prechromomycin B.

Initial Characterization of CmmOIV. CmmOIV is homologous to the well-studied MtmOIV oxygenase from the mithramycin biosynthetic pathway (*27*, *31*, *32*). Both enzymes are FAD- and NADPH-dependent and require molecular oxygen. Crystallography studies of MtmOIV showed the enzyme acts as a dimer with both FAD binding sites filled with an FAD moiety, although the biochemical studies showed a 2:1 protein:FAD ratio (*27*). Like MtmOIV, CmmOIV catalyzes the insertion of an oxygen atom into the fourth ring of a so far not clearly identified prechromomycin B-type compound, which eventually converts a tetracyclic substrate into a tricyclic product. This breakage of the fourth ring catalyzed by CmmOIV is a key reaction, because it goes hand in hand with the establishment of the antitumor activity found for chromomycin.

The molecular weight of CmmOIV was calculated to be 54211.9844. Figure 3A shows purified CmmOIV, with the His_6 tag removed running at approximately 55000 on a 10 to 16% SDS−PAGE gradient gel (Bio-Rad). In all further experiments, the His_6 tag was left uncleaved, and a separate molecular weight calculation indicated a molecular weight of 56012.9023 for the His_6-tagged enzyme. A dimer of the His_6-tagged protein was calculated to have a molecular weight of 112026. To verify that CmmOIV, like MtmOIV, also acts as a dimer, we ran purified CmmOIV under native conditions on a 10% native PAGE gel, and the protein ran at a molecular weight of approximately 120000, indicative of the dimer (Figure 3B). To confirm that CmmOIV is in fact a dimer, we also ran the protein across a gel filtration column under native conditions (Figure 3C,D), using a series of five proteins as molecular weight standards (see Experimental Procedures) and blue dextran to estimate the void volume. Gel filtration experiments indicated a molecular weight of 118111, further confirming the dimeric nature of CmmOIV.

CmmOIV Reaction Optimization. Prior to characterization of CmmOIV, we first needed to optimize the reaction conditions used to assay enzymatic activity. The CmmOIV reaction was first tested in the presence or absence of 100 μM FAD (data not shown). At pH 8.5 and 100 μM substrate, approximately 30% of the amplitude was lost without addition of FAD to the reaction mixture (data not shown). This result indicates that the FAD binding is noncovalent and the FAD binding sites on CmmOIV are not completely filled prior to initiation of the reaction. Further experiments measuring the FAD concentration following enzyme purification resulted in an FAD:CmmOIV ratio of only 1:2 to 1:4. Incubation of CmmOIV with FAD on ice increased the FAD:CmmOIV ratio, but not consistently to 1:1.

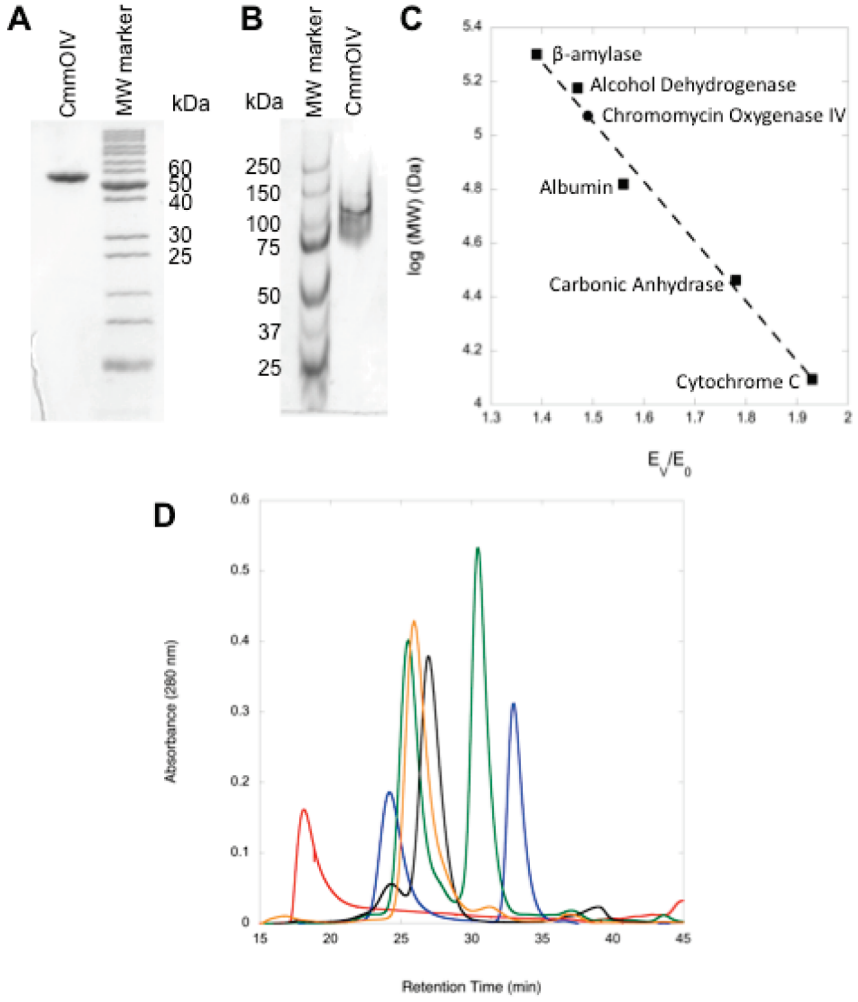

FIGURE 3: CmmOIV molecular weight under denaturing and native conditions. (A) CmmOIV runs at 56000 on standard SDS−PAGE. (B) On a native gel, CmmOIV shifts to 120000, indicating CmmOIV is dimeric in solution. (C) Gel filtration column using five proteins as standards (■) showing CmmOIV (●) with an E_v/E_0 ratio of 1.49, where E_v is the elution volume and E_0 is the void volume measured by elution of blue dextran. This ratio yields a molecular weight of 118111, confirming that CmmOIV is dimeric in solution. (D) FPLC chromatogram traces of protein standards and CmmOIV measured at 280 nm: blue dextran (red), cytochrome *c* and *β*-amylase (blue), carbonic anhydrase and alcohol dehydrogenase (green), CmmOIV (orange), and albumin (black).

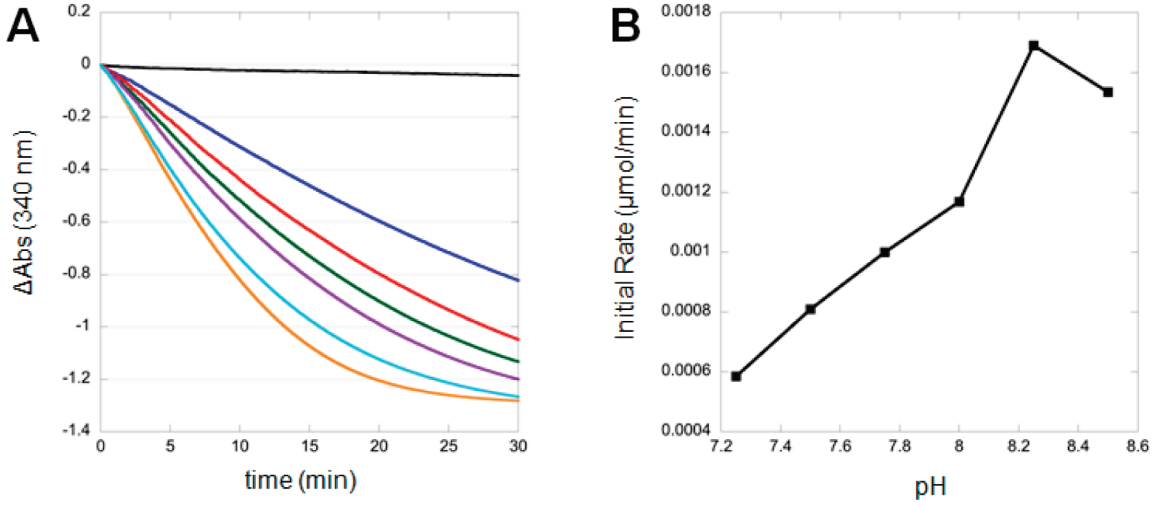

FIGURE 4: pH optimization of the CmmOIV reaction. (A) Comparison of NADPH oxidation, measured by decreased absorbance at 340 nm, from CmmOIV turnover of **6** in 0.1 mM Tris-HCl buffer at pH 7.25 (blue), pH 7.5 (red), pH 7.75 (green), pH 8.0 (purple), pH 8.25 (orange), and pH 8.5 (cyan). Each line represents an average of three measured spectra. The blank (black) represents NADPH oxidation in the absence of enzyme. (B) Initial rates of NADPH oxidation measured from the turnover of **6** by CmmOIV clearly indicate maximal turnover at pH 8.25.

These data determined that supplementing each reaction mixture with 100 μM FAD eliminated any artificial variations in enzyme activity stemming from FAD concentration. The pH of the CmmOIV reaction with **6** as the substrate was optimized using

100 mM Tris buffers with varying pH (Figure 4). The initial rate of these reactions was measured, and a maximum was reached at pH 8.25. Also, NADH and NADPH were both evaluated as cosubstrates for the CmmOIV reaction by determining initial rates in the presence of each cosubstrate. Like those of MtmOIV, CmmOIV reaction rates were greatly reduced in the presence of NADH compared to NADPH, and overall reaction amplitudes decreased up to 30% (data not shown). Additionally, $K_{M,6}$ with NADH as the cosubstrate decreased more than 10-fold compared to $K_{M,6}$ in the presence of NADPH, confirming that NADPH is the preferred cosubstrate (Table 3).

CmmOIV Steady-State Kinetics. To identify the natural substrate of CmmOIV and to delineate the sequence of the terminal reactions of the chromomycin A_3 biosynthetic pathway, we determined the steady-state kinetic parameters of the CmmOIV enzyme with three of the isolated compounds available from the CmmOIV mutant strain: **6**, **11**, and **12**. Surprisingly, CmmOIV enzyme efficiency decreased when it reacted with **12** compared to when it reacted with **6** and further decreased when it reacted with **11** (Figure 5 and Table 3). Although compounds **6** and **12** vary by only a single acetyl group existing in sugar A of **6**, the change in the rate and amplitude of the reaction is significant. It appears that both acetyl groups are required for full enzymatic activity of CmmOIV and that the loss of one acetyl group negatively affects the turnover rate. The diketo substrate **11** lost nearly all CmmOIV activity compared to **6**, suggesting either that the keto groups play an inhibitory role or that the lack of decoration at the sugar residues prevents substrate binding or CmmOIV turnover.

DISCUSSION

In summary, none of the compounds accumulated by the CmmOIV-minus mutant were identified as the expected substrate, prechromomycin B **5** (Scheme 1). This was surprising as the MtmOIV-minus mutant strain from the sister mithramycin biosynthetic pathway yielded predominantly premithramycin B **4** along with minor amounts of 3A-deolivosyl-premithramycin B (*30*). The fact that **5** does not accumulate upon CmmOIV inactivation indicates that the O-acetylation and O-methylation reactions occur fast, possibly to stabilize an otherwise unstable intermediate. Premithramycin B **4** was clearly identified as the MtmOIV substrate and 3A-deolivosyl-premithramycin B as its immediate biosynthetic precursor. Ignoring the minor products **10** and **11** of the CmmOIV inactivation, which were found in only miniscule amounts, we found that accumulation of fully functionalized **6** as the major compound accompanied by minor amounts of the monoacetylated compound **12** suggests **6** is the CmmOIV substrate and **12** is its immediate precursor, to match perfectly the findings of the chromomycin pathway with those established for the mithramycin biosynthetic pathway. Investigations with purified CmmOIV were designed to further substantiate this possible revision of the late chromomycin A_3 biosynthetic pathway. The previously favored CmmOIV substrate, prechromomycin B **5**, was never isolated and apparently does not accumulate upon CmmOIV inactivation. Thus, although previous work suggested a terminal role for the tailoring enzymes, CmmA and CmmMIII (*8*), our findings here now suggest that it is more likely that CmmOIV naturally acts on a fully O-acetyl- and O-methyl-functionalized substrate.

Menéndez et al. (*8*, *26*) previously showed that the acetyl groups of chromomycin A_3 contribute to its antitumor properties, and it was shown by Chakrabarti et al. (*22*) that the O-acetyl groups help to stabilize the DNA interaction of the chromomycin–Mg^{2+} complex. Our work presented here, the inactivation and initial interrogation of CmmOIV, revealed the fully functionalized substrate **6** to be the major accumulating product of the CmmOIV-minus mutant strain, followed by minor amounts of the monoacetylated substrate **12**, diketo compound **11**, and four-sugar compound **10**. Fully characterizing the steady-state kinetics of these accumulated compounds with CmmOIV clearly indicates that a completely acetylated and methylated prechromomycin **6** is preferred by this critical bottleneck oxygenase over its nondecorated and incompletely acetylated precursors **11** and **12**, respectively. This in turn would suggest that the sugar decoration (O-acetylation and O-methylation) reactions, previously believed to occur at the very end of the chromomycin A_3 biosynthesis, indeed take place prior to the CmmOIV reaction. Thus, the biosynthetic **5**→**6**→**9** sequence is more likely than the previously suggested **5** → **8** → **9** sequence (see Scheme 1). We are hopeful

Table 3: Steady-State Kinetic Parameters of CmmOIV with Various Substrates

substrate	K_M (μM)	k_{cat} (s^{-1})	k_{cat}/K_M (mM s^{-1})
NADPH			
6	5.74 ± 0.57	0.29 ± 0.01	50.5
12	30.21 ± 3.38	0.25 ± 0.01	8.3
11	nd[a]	0.025 ± 0.004	nd[a]
NADH			
6	79.58 ± 25.27	0.29 ± 0.03	3.64

[a]Not determined.

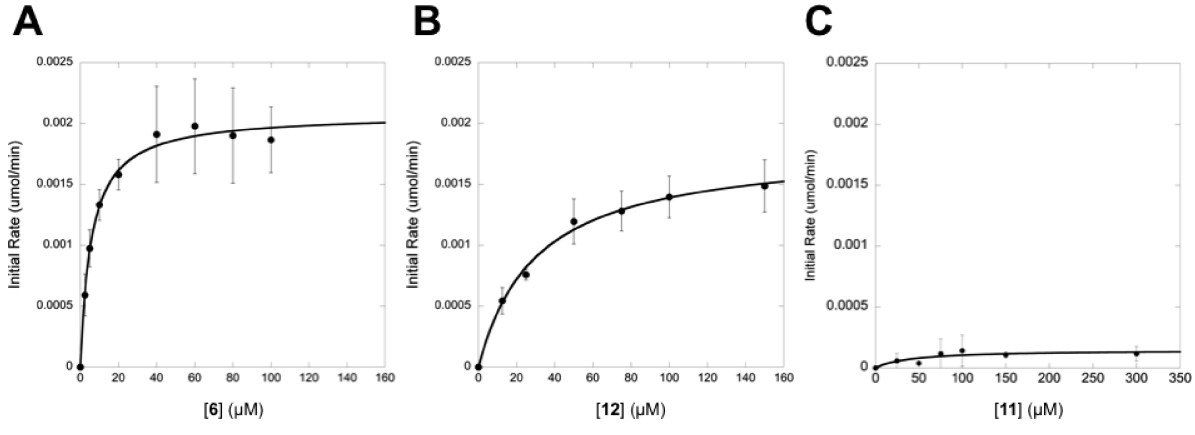

FIGURE 5: CmmOIV reactions fitted with the Michaelis–Menten equation. Initial rates (micromoles per minute) of NADPH oxidation from CmmOIV turnover of substrates: (A) **6**, (B) **12**, and (C) **11**.

crystallization of CmmOIV (currently under investigation) will shed further light on this question.

ACKNOWLEDGMENT

We thank Professor Steven van Lanen for the use of an UV spectrophotometer to measure the kinetics of CmmOIV and of an FPLC system for gel filtration chromatography. We also acknowledge the use of the instruments of the University of Kentucky NMR core facility, and Dr. Jack Goodman (University of Kentucky mass spectroscopy facilities) is acknowledged for the high-resolution mass spectra.

SUPPORTING INFORMATION AVAILABLE

Insertional inactivation of the gene encoding CmmOIV and tables with NMR data for compounds **6**, **11**, and **12**. This material is available free of charge via the Internet at http://pubs.acs.org.

REFERENCES

1. Skarbek, J. D., and Speedie, M. K. (1981) Antitumor antibiotics of the aureolic acid group: Chromomycin A3, mithramycin A, and olivomycin A. In Antitumor compounds of natural origin: Chemistry and biochemistry (Aszalos, A., Ed.) pp 191−235, CRC Press, Boca Raton, FL.
2. Lombó, F., Menendez, N., Salas, J. A., and Méndez, C. (2006) The aureolic acid family of antitumor compounds: Structure, mode of action, biosynthesis, and novel derivatives. *Appl. Microbiol. Biotechnol. 73*, 1–14.
3. Majee, S., Sen, R., Guha, S., Bhattacharyya, D., and Dasgupta, D. (1997) Differential Interactions of the Mg^{2+} Complexes of Chromomycin A_3 and Mithramycin with Poly(dG-dC)·Poly(dC-dG) and Poly(dG)·Poly(dC). *Biochemistry 36*, 2291–2299.
4. Silva, D. J., Goodnow, R., Jr., and Kahne, D. (1993) The sugars in chromomycin A3 stabilize the Mg^{2+}-dimer complex. *Biochemistry 32*, 463–471.
5. Jayasuriya, H., Lingham, R. B., Graham, P., Quamina, D., Herranz, L., Genilloud, O., Gagliardi, M., Danzeisen, R., Tomassini, J. E., Zink, D. L., Guan, Z. Q., and Singh, S. B. (2002) Durhamycin A, a potent inhibitor of HIV Tat transactivation. *J. Nat. Prod. 65*, 1091–1095.
6. Bianchi, N., Osti, F., Rutigliano, C., Corradini, F. G., Borsetti, E., Tomassetti, M., Mischiati, C., Feriotto, G., and Gambari, R. (1999) The DNA-binding drugs mithramycin and chromomycin are powerful inducers of erythroid differentiation of human K562 cells. *Br. J. Haematol. 104*, 258–265.
7. Devi, P. G., Chakraborty, P. K., and Dasgupta, D. (2009) Inhibition of a Zn(II)-containing enzyme, alcohol dehydrogenase, by anticancer antibiotics, mithramycin and chromomycin A3. *J. Biol. Inorg. Chem. 14*, 347–359.
8. Menéndez, N., Nur-e-Alam, M., Braña, A. F., Rohr, J., Salas, J. A., and Méndez, C. (2004) Tailoring modification of deoxysugars during biosynthesis of the antitumour drug chromomycin A by *Streptomyces griseus* ssp. *griseus*. *Mol. Microbiol. 53*, 903–915.
9. Menéndez, N., Nur-e-Alam, M., Braña, A. F., Rohr, J., Salas, J. A., and Méndez, C. (2004) Biosynthesis of the antitumor chromomycin A3 in *Streptomyces griseus*: Analysis of the gene cluster and rational design of novel chromomycin analogs. *Chem. Biol. 11*, 21–32.
10. Menéndez, N., Nur-e-Alam, M., Fischer, C., Braña, A. F., Salas, J. A., Rohr, J., and Méndez, C. (2006) Deoxysugar Transfer during Chromomycin A3 Biosynthesis in *Streptomyces griseus* subsp. *griseus*: New Derivatives with Antitumor Activity. *Appl. Environ. Microbiol. 72*, 167–177.
11. Montanari, A., and Rosazza, J. P. (1990) Biogenesis of chromomycin A3 by *Streptomyces griseus*. *J. Antibiot. 43*, 883–889.
12. Aich, P., and Dasgupta, D. (1990) Role of Mg^{2+} in the mithramycin-DNA interaction: Evidence for two types of mithramycin-Mg^{2+} complex. *Biochem. Biophys. Res. Commun. 173*, 689–696.
13. Majee, S., Dasgupta, D., and Chakrabarti, A. (1999) Interaction of the DNA-binding antitumor antibiotics, chromomycin and mithramycin with erythroid spectrin. *Eur. J. Biochem. 260*, 619–626.
14. Mir, M. A., Majee, S., Das, S., and Dasgupta, D. (2003) Association of chromatin with anticancer antibiotics, mithramycin and chromomycin A3. *Bioorg. Med. Chem. 11*, 2791–2801.
15. Silva, D. J., and Kahne, D. E. (1993) Studies of the 2:1 Chromomycin A_3-Mg^{2+} Complex in Methanol: Role of the Carbohydrates in Complex Formation. *J. Am. Chem. Soc. 115*, 7962–7970.
16. Mir, M. A., and Dasgupta, D. (2001) Association of the Anticancer Antibiotic Chromomycin A3 with the Nucleosome: Role of Core Histone Tail Domains in the Binding Process. *Biochemistry 40*, 11578–11585.
17. Keniry, M. A., Banville, D. L., Simmonds, P. M., and Shafer, R. H. (1993) Nuclear magnetic resonance comparison of the binding sites of mithramycin and chromomycin on the self-complementary oligonucleotide $d(ACCCGGGT)_2$. Evidence that the saccharide chains have a role in sequence specificity. *J. Mol. Biol. 231*, 753–767.
18. Keniry, M. A., Owen, E. A., and Shafer, R. H. (2000) The three-dimensional structure of the 4:1 mithramycin:$d(ACCCGGGT)_2$ complex: Evidence for an interaction between the E saccharides. *Biopolymers 54*, 104–114.
19. Hou, M. H., Robinson, H., Gao, Y. G., and Wang, A. H. (2004) Crystal structure of the $[Mg^{2+}$-(chromomycin $A3)_2]$-$d(TTGGCCAA)_2$ complex reveals GGCC binding specificity of the drug dimer chelated by a metal ion. *Nucleic Acids Res. 32*, 2214–2222.
20. Hou, M. H., Lu, W. J., Lin, H. Y., and Yuann, J. M. (2008) Studies of sequence-specific DNA binding, DNA cleavage, and topoisomerase I inhibition by the dimeric chromomycin A3 complexed with Fe(II). *Biochemistry 47*, 5493–5502.
21. Gao, X., and Patel, D. J. (1989) Solution structure of the chromomycin-DNA complex. *Biochemistry 28*, 751–762.
22. Chakrabarti, S., Bhattacharyya, B., and Dasgupta, D. (2002) Interaction of Mithramycin and Chromomycin A_3 with $d(TAGCTAGCTA)_2$: Role of Sugars in Antibiotic-DNA Recognition. *J. Phys. Chem. B 106*, 6947–6953.
23. Chakrabarti, S., Bhattacharyya, D., and Dasgupta, D. (2001) Structural basis of DNA recognition by anticancer antibiotics, chromomycin A_3, and mithramycin: Roles of minor groove width and ligand flexibility. *Biopolymers 56*, 85–95.
24. Chakrabarti, S., and Dasgupta, D. (2001) Interactions of chromomycin A3 and mithramycin with the sequence $d(TAGCTAGCTA)_2$. *Indian J. Biochem. Biophys. 38*, 64–70.
25. Chakrabarti, S., Mir, M. A., and Dasgupta, D. (2001) Differential interactions of antitumor antibiotics chromomycin A_3 and mithramycin with $d(TATGCATA)_2$ in presence of Mg^{2+}. *Biopolymers 62*, 131–140.
26. Menéndez, N., Brana, A. F., Salas, J. A., and Mendez, C. (2007) Involvement of a chromomycin ABC transporter system in secretion of a deacetylated precursor during chromomycin biosynthesis. *Microbiology 153*, 3061–3070.
27. Beam, M. P., Bosserman, M. A., Noinaj, N., Wehenkel, M., and Rohr, J. (2009) Crystal structure of Baeyer-Villiger monooxygenase MtmOIV, the key enzyme of the mithramycin biosynthetic pathway. *Biochemistry 48*, 4476–4487.
28. Fernandez-Lozano, M. J., Remsing, L. L., Quiros, L. M., Braña, A. F., Fernandez, E., Sanchez, C., Méndez, C., Rohr, J., and Salas, J. A. (2000) Characterization of two polyketide methyltransferases involved in the biosynthesis of the antitumor drug mithramycin by *Streptomyces argillaceus*. *J. Biol. Chem. 275*, 3065–3074.
29. Olano, C., Gómez, C., Pérez, M., Palomino, M., Pineda-Lucena, A., Carbajo, R. J., Braña, A. F., Méndez, C., and Salas, J. A. (2009) Deciphering biosynthesis of the RNA polymerase inhibitor streptolydigin and generation of glycosylated derivatives. *Chem. Biol. 16*, 1031–1044.
30. Prado, L., Fernandez, E., Weissbach, U., Blanco, G., Quiros, L. M., Brana, A. F., Méndez, C., Rohr, J., and Salas, J. A. (1999) Oxidative cleavage of premithramycin B is one of the last steps in the biosynthesis of the antitumor drug mithramycin. *Chem. Biol. 6*, 19–30.
31. Rodriguez, D., Quiros, L. M., Braña, A. F., and Salas, J. A. (2003) Purification and characterization of a monooxygenase involved in the biosynthetic pathway of the antitumor drug mithramycin. *J. Bacteriol. 185*, 3962–3965.
32. Gibson, M., Nur-e-Alam, M., Lipata, F., Oliveira, M. A., and Rohr, J. (2005) Characterization of Kinetics and Products of the Baeyer-Villiger Oxygenase MtmOIV, the Key Enzyme of the Biosynthetic Pathway toward the Natural Product Anticancer Drug Mithramycin from *Streptomyces argillaceus*. *J. Am. Chem. Soc. 127*, 17594–17595.